

Special Section:

Fire in the Earth System

Key Points:

- Peat burning in the Mezzano Lowland is a process active since wetland reclamation and variously affects the soil structure and carbon content
- The main carbon loss occurs in the depth interval 10–70 cm, where temperature up to 750°C is recorded
- The process induces negative effects to surrounding environment, agriculture activities and possibly also human health

Supporting Information:

Supporting Information may be found in the online version of this article.

Correspondence to:

G. Bianchini,
bncglc@unife.it

Citation:

Natali, C., Bianchini, G., Cremonini, S., Salani, G. M., Vianello, G., Brombin, V., et al. (2021). Peat soil burning in the Mezzano Lowland (Po Plain, Italy): Triggering mechanisms and environmental consequences. *GeoHealth*, 5, e2021GH000444. <https://doi.org/10.1029/2021GH000444>

Received 23 APR 2021



Accepted 9 JUL 2021

Author Contributions:

Conceptualization: Claudio Natali, Stefano Cremonini, Gilmo Vianello
Data curation: Claudio Natali, Livia Vittori Antisari

© 2021. The Authors. GeoHealth published by Wiley Periodicals LLC on behalf of American Geophysical Union. This is an open access article under the terms of the [Creative Commons Attribution-NonCommercial-NoDerivs License](https://creativecommons.org/licenses/by-nc-nd/4.0/), which permits use and distribution in any medium, provided the original work is properly cited, the use is non-commercial and no modifications or adaptations are made.

Peat Soil Burning in the Mezzano Lowland (Po Plain, Italy): Triggering Mechanisms and Environmental Consequences

Claudio Natali^{1,2} , Gianluca Bianchini^{2,3} , Stefano Cremonini⁴, Gian Marco Salani³, Gilmo Vianello⁵, Valentina Brombin^{2,3}, Mattia Ferrari^{1,3}, and Livia Vittori Antisari⁵

¹Department of Earth Sciences, University of Florence, Florence, Italy, ²Institute of Environmental Geology and Geoenvironment of the Italian National Research Council (CNR-IGAG), Montelibretti, Italy, ³Department of Physics and Earth Sciences, University of Ferrara, Ferrara, Italy, ⁴Department of Biological, Geological and Environmental Sciences, University of Bologna, Bologna, Italy, ⁵Department of Agricultural and Food Sciences, University of Bologna, Bologna, Italy

Abstract The effects of peat burning on organic-rich agricultural soils of the Mezzano Lowland (NE Italy) were evaluated on soil profiles variously affected by smoldering. Profiles were investigated for pH, electrical conductivity, bulk density, elemental and isotopic composition of distinct carbon (and nitrogen) fractions. The results suggest that the horizons affected by carbon loss lie at depths 10–70 cm, where the highest temperatures are developed. We suggest that the exothermal oxidation of methane (mediated by biological activity) plays a significant role in the triggering mechanism. In the interested soils we estimated a potential loss of Soil Organic Carbon of approximately 110 kg m⁻² within the first meter, corresponding to 580 kg CO₂ m⁻³. The released greenhouse gas is coupled with a loss of soil structure and nutrients. Moreover, the process plausibly triggers mobility of metals bound in organometallic complexes. All these consequences negatively affect the environment, the agricultural activities and possibly also health of the local people.

Plain Language Summary Peat soils are formed by accumulation of organic matter and represent a carbon sink. Unfortunately, they are often affected by burning as the organic matter can fuel combustion for a long time, ultimately releasing carbon dioxide and other greenhouse gases, and particulate matter (PM). It is not clear how peat burning ignites and spreads. This study investigates the trigger mechanisms and effects of peat burning in the Mezzano Lowland (NE Italy). For this purpose, pH, electrical conductivity, bulk density and carbon elemental and isotopic compositions of Mezzano soil profiles variously affected by peat burning have been investigated. The results suggest that the burning doesn't propagate from surface and that the horizons affected by carbon loss lie at depths 10–70 cm, with temperatures up to 750°C. The process appears spontaneous, probably due to multiple factors such as drying, biological activity and exothermal oxidations. We estimated a loss of soil carbon of approximately 110 kg for square meter, corresponding to a release of 580 kg of CO₂ for cubic meter of burnt soil. This carbon loss and the consequent release of gas and PM negatively affect the environment, the agricultural activities and possibly also the health of the local people.

1. Introduction

Peat soils are organic-rich sedimentary deposits that formed by the accumulation of biomass in water-saturated conditions. Peat bogs minimize organic matter decomposition, and serve as important carbon reservoir worldwide (Belyea & Malmer, 2004; Natali, Bianchini, Vittori Antisari, Natale, & Tessari, 2018; Rein, 2015; Smith et al., 2004). Globally, peat soils contain one-third of the world's soil carbon; their carbon budget exceeds that of the forests, and is comparable to that of the atmosphere (Joosten & Clarke, 2002).

Unfortunately, peat soils are episodically affected by burning, as soil organic matter (SOM) can fuel and sustain the burning process for a long time (Moreno et al., 2011; Rein, 2015). According to the literature, peat smoldering can reach maximum temperatures of 700°C that, although lower than that of flaming combustion (1,500–1,800°C, Rein, 2009; Rein et al., 2008), progressively degrades SOM (Kreye et al., 2011).

Investigation: Claudio Natali, Stefano Cremonini, Gian Marco Salani, Gilmo Vianello, Mattia Ferrari

Methodology: Claudio Natali, Gian Marco Salani, Valentina Brombin

Supervision: Gilmo Vianello, Livia Vittori Antisari

Writing – review & editing: Gianluca Bianchini, Valentina Brombin

Several studies have indicated that peat burning is triggered by surface fires that progressively propagates downward in low oxygen conditions (Joosten & Clarke, 2002), as in the cases of peat fires in Indonesia (Boehm et al., 2001; Page et al., 2002; Usup et al., 2004) and Florida (Monroe et al., 2009; Watts & Kobziar, 2013). Noteworthy, these processes deserve particular attention, as they produce more greenhouse emissions than vegetation fires and become progressively frequent under drought conditions (Langmann & Heil, 2004). Considering that future climate change scenarios predict more frequent and severe drought events in many areas worldwide (IPCC, 2007), soil fires need to be better understood to manage and mitigate their detrimental effects (Abram et al., 2021), which can impact also the human health (Uda et al., 2019).

In Italy, peats (and associated soils) are mainly distributed in the north and were generated in alluvial basins from the late Würm (late Pleistocene) to the Holocene (Martinelli et al., 2015).

This paper presents a case study of peat burning in the Mezzano Lowland (ML; Figure 1), a reclaimed coastal wetland located in the easternmost Po Plain, which is located in northern Italy (Di Giuseppe et al., 2014a, 2014b). This area is renowned for peat burning since historical times (Cremonini et al., 2008; Martinelli et al., 2015), and is characterized by peat deposits exposed to the Mediterranean climate with frequent and persistent droughts (Marchina et al., 2017, 2019). To assess the effects of burning, we applied an analytical technique based on the distinctive thermal stability of the various carbon bearing-phases (Mörchen et al., 2019; Natali et al., 2020; Zethof et al., 2019, 2020) as well as isotope ratio mass spectrometry (Natali, Bianchini, & Vittori Antisari, 2018). With the obtained results we provide constraints on the effects of burning in the surrounding environment, evaluating the smoldering combustion effects on the local soil carbon stock.

2. Geomorphological Features

The Po Plain is a large alluvial basin filled by sediments eroded from the Alps and the Apennines, which have been transported and deposited by the Po River (Amorosi et al., 2002; Garzanti et al., 2012; Bianchini et al., 2002, 2012, 2013). In particular, the ML represents the terminal (deltaic) portion of the Po River catchment close to the Adriatic Sea and has been historically characterized by wetlands reclaimed ca. 60–70 years ago. The ML soils therefore evolved from alluvial and deltaic lacustrine sediments (Di Giuseppe et al., 2014a, 2014b; Natali, Bianchini, Vittori Antisari, Natale, & Tessari, 2018; Simeoni & Corbau, 2009; Stefani & Vincenzi, 2005) and are organic-rich, including repeated levels of peats (Miola et al., 2006). The total ML peat volume is estimated to be $177 \times 10^6 \text{ m}^3$ (Cremonini et al., 2008). The ML peat soils are also renowned for methane seepage and local thermal anomalies recorded down to a depth of 1 m (Bonzi et al., 2017). Analogous thermal anomalies have been observed in other parts of the Po Plain and ascribed to the exothermal oxidation of CH_4 mediated by biochemical processes (Capaccioni et al., 2015).

3. Materials and Methods

3.1. Investigated Samples

The sub-rectangular sampling area extended from $44^\circ 41' 17.08'' \text{N}$, $12^\circ 00' 09.34'' \text{E}$ (upper left corner) to $44^\circ 40' 35.45'' \text{N}$, $12^\circ 00' 51.96'' \text{E}$ (lower right corner). It was investigated in July 2018 (Figure 2), when the area experienced ongoing peat fires at its southern edge. The northern edge was instead affected by fires in the past (Martinelli et al., 2015). Each peat fire event was confined to a subcircular area of approximately 3–4 m in diameter, characterized by the absence of vegetation (Figure 1b). Five trenches, approximately 2 m long, 1 m wide and 1 m deep, were dug to access the soil profile for inspection, and the well-exposed sides of the pits were observed carefully to determine the different soil horizons. Soil profile TOR1 was the only one dug in the sector affected by the active fire, while other two profiles (TOR2 and TOR3, Figure 1b) were dug in the sector affected by past fire events. They were characterized by horizons having reddish color (Figure 1c), consisting of very fine ashy particles that obliterated the original structural characteristics. Other two profiles (TOR4 and TOR5) were dug in sectors of the investigated area not interested by peat smoldering, to perceive the original soil condition preceding the burning processes.

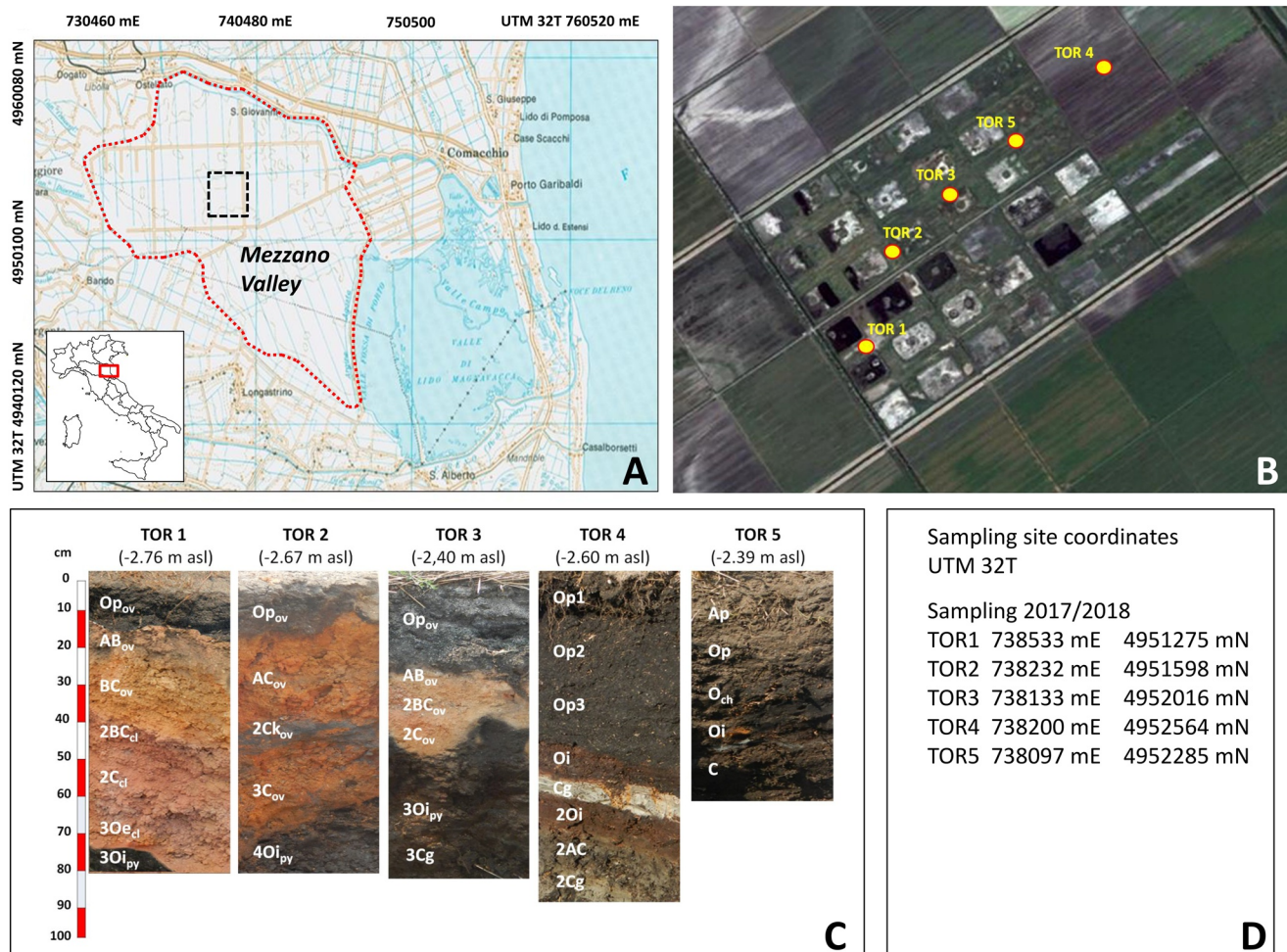


Figure 1. (a) Geographic location of the study area (black dashed line) within the the Mezzano Lowland (red dashed line) in the easternmost Padanian plain (Northern Italy), facing the Adriatic Sea. (b) Satellite image (Google Earth, year 2010) showing the study area and the sampling locations of the investigated soil profiles. Note the presence of several fired elliptical areas. (c) Photographs of the fired (TOR1, TOR2, TOR3) and non-fired (TOR4 and TOR5) soil profiles and (d) relative geographic coordinates.

Thirty-four representative samples (of about 1–2 kg) were collected from horizons of the soil profiles TOR1–TOR3 variously affected (F) by peat burning, and soil profiles TOR4 and TOR5 unaffected (NF) by peat burning.

The soil horizons were described according to Schoeneberger et al. (2012). We attributed specific suffixes to the horizons where peat smoldering induced different effects due to the temperature increase; for example, Oipy was attributed to the pyrolyzed organic horizon with peat carbonization, 2Ccl to the calcined mineral horizon, and ABo_v to the overheated organo-mineral horizon.

3.2. Experimental Firing of NF Soil Profiles

In the laboratory, we burnt samples from horizons of the profile TOR4 which is located in a sector unaffected by natural fire, to simulate the processes and to evaluate the thermal transformation of soil samples induced by peat burning, following the method by Gonzalez-Vila (2003). Thermal heating was applied for 12 h at different temperatures using an electric muffle. Three replicates were prepared using 100-ml porcelain crucibles, each containing 20 g of soil sample. After isothermal heating at 105, 200, 400, and 600°C, we used 4 g of heated soil to quantitatively determine the different carbon fractions.



Figure 2. Pictures showing an ongoing peat fire phenomenon in the neighbors of profile TOR1. (a and c) Note that the inner part of the fired elliptical area is depressed with respect to the neighbors, and (d) that smoke developed at depth escapes from the superficial layer of unburned peat.

3.3. pH, Electrical Conductivity and Bulk Density

To determine the soil physicochemical parameters, the samples were air-dried and sieved through a 2-mm mesh sieve. Soil pH was measured by potentiometric titration on a 1:2.5 (w/v) soil:distilled water suspension with a Crison pH meter. Soil electrical conductivity (EC), expressed as deciSiemens per meter (dS m^{-1}), was obtained on a 1:2.5 (w/v) aqueous suspension filtered with a Whatman® 42 filter paper using an Orion conductivity-meter. Undisturbed soil samples collected in the steel cylinders of known volume were weighed after drying at 105°C for 24 h to calculate the bulk density (BD), which is the weight of dry soil divided by the total soil volume expressed in grams per cubic centimeter (g cm^{-3}).

3.4. Temperature-Dependent Differentiation of Total Carbon

We used the Elementar SoliTOC Cube elemental analyzer, in compliance with the DIN 19539 standard, to carry out the temperature-dependent differentiation of total carbon (TC) in the investigated soil samples. This method is also known as “smart combustion” (Zethof et al., 2019). Powdered samples were loaded in stainless steel crucibles and placed in an 80-position autosampler. The crucibles were picked up by a stainless steel arm and placed in the dynamically heated portion of the combustion column at an initial temperature of 60°C . The analytical run required approximately 1,600 s and involved a three-step heating of the samples to 400, 600, and 900°C with holding time of 230, 120, and 150 s, respectively. The CO_2 produced during the sample combustion was collected by two dedicated traps and sent to an IR detector for the continuous measurement of carbon. The DIN 19539 standard involves the separation and analysis of two oxidizable soil carbon pools with different thermal stabilities (i.e., thermally labile organic carbon— TOC_{400} —stripped out at temperatures below 400°C , and residual oxidizable carbon—ROC—at temperatures of 500 – 600°C) and one carbon pool derived from the thermal breakdown of carbonate minerals at 650 – 850°C (total inorganic carbon (TIC)). At the end of the analytical run, an internal fan reset the temperature of the dynamically heated portion of the column to 60°C . The same analytical device was used by Natali et al. (2020) to quantify the carbon pools in a soil sample set characterized by substantial textural and geochemical variability. They defined TOC as the sum of the TOC_{400} and ROC organic carbon pools. For the samples considered in this study, analyses were performed in triplicate, and the data are expressed with the average and the standard deviation. Further constraints were provided by an analytical cross-check obtained analyzing the same samples with independent methods (see Table S1).

3.5. Carbon Isotope Analysis by EA-IRMS

We used the Elementar Vario MICRO Cube elemental analyzer (EA) coupled with the IsoPrime100 isotope ratio mass spectrometer (IRMS) in the continuous-flow mode. Powdered samples were weighed and wrapped in tin capsules. These capsules allowed loading of up to 40 mg of sample material and were subsequently introduced into the Vario MICRO Cube autosampler for the analysis. Flash combustion occurred in a sealed quartz tube filled with copper oxide grains in an excess of high-purity O₂ gas (grade purity 6). The carbon and nitrogen gaseous species were released by the burnt samples and were transferred to another tube maintained at 550°C. This tube contained chips of native copper, which reduced the nitrogen oxides (NO_x) to N₂. The formed CO₂ and N₂ gases were carried by He (grade purity 5) gas flow within a trap containing Sicapent® to remove H₂O. The CO₂ and N₂ gases were finally separated by a temperature programmable desorption column, and were quantitatively determined using a thermo-conductivity detector (TCD).

The CO₂ gas was conveyed to the IRMS to determine carbon isotopic ratios. The detected isotopic masses of the sample were compared to those of the reference CO₂ (grade purity 5) gas. The reference gas was previously calibrated using various reference materials such as the limestone JLS-1 (Kusaka & Nakano, 2014), the peach leaves NIST SRM1547 (Dutta et al., 2006), the Carrara Marble (calibrated at the Institute of Geoscience and Georesources of the Italian National Research Council), the Jacupiranga carbonatite (Beccaluva et al., 2017; Santos & Clayton, 1995) and the synthetic sulfanilamide provided by Isoprime Ltd. Mass peaks were recalculated as isotopic ratios using the Ion Vantage software package.

Elemental precision was estimated by repeated standard analyses. Accuracy was evaluated by comparing the reference and measured values. Both parameters were approximately 5% of the absolute measured value, but uncertainty increased for contents approaching the detection limit (0.001 wt%). The concentrations obtained with this instrument and those obtained with the SoliTOC described in the previous section are in excellent agreement (see comparison in Table S1).

Carbon isotope ratios were expressed with the δ notation in per mil (‰), relative to the international Vienna Pee Dee Belemnite isotope standard (Gonfiantini et al., 1995). The $\delta^{13}\text{C}$ values were characterized by an average standard deviation of $\pm 0.1\%$, as defined by the repeated analyses of the above-mentioned standards.

3.6. Statistical Analysis

The statistical analysis was conducted by R (R Core Team, 2017). The analysis of variance (ANOVA test) was applied to every variable in order to determine the statistical differences between the different soil profiles. The PCA was subsequently applied to examine differences in elemental and isotopic parameters between F and NF soil profiles (package “FactoMineR” (Le et al., 2008); package “factoextra” (Kassambara, 2017)).

4. Results

4.1. pH, Electrical Conductivity and Bulk Density

The physicochemical parameters of the soil horizons from the five investigated soil profiles are shown in Table 1. The pH values generally decreased with depth in all investigated profiles, but the F and NF profile trends (and average values) are characterized by significant differences. The pH of the NF profiles (TOR4 and TOR5) varied from 2.4 (TOR4, 2AC, 63–75 cm depth) to 7.6 (TOR5, Op, 22–30 cm depth), with average pH value of 5.5. The F profiles (TOR1–TOR3) displayed a comparable pH range, varying from 3.3 (TOR3, Cg, 70–90 cm depth) to 8.3 (TOR2, 3Cov, 43–65 cm depth), with an average of pH value of 6.6. A marked increase in pH characterized the horizons at intermediate depths (35–70 cm) of the F profiles, whereas a slight pH decrease was observed in the NF profiles at comparable depths. EC of the F profiles had an average of 8.1 dS m⁻¹ generally higher than what observed in NF profiles (average 5.3 dS m⁻¹). Noteworthy, EC in F profiles presented an inverse relationship with depth, with a general decrease in EC at depths of 35–70 cm. The BD of the F profiles was heterogeneous, varying between 0.51 and 1.19 g cm⁻³, with the lowest values recorded between depths of 12 cm (TOR2, ACov, 12–38 cm depth) and 43 cm (TOR1, BCov, 30–43 cm depth). The BD of the NF profiles (average 1 g cm⁻³) generally increased with depth and was higher than that in the F profiles (average 0.8 g cm⁻³) that showed the lowest values in the 30–70 cm depth range.

Table 1
Physicochemical Parameters, Carbon Fractions (and Isotope Composition) and Nitrogen of the Soil Profiles Variably Affected (TOR1, TOR2, TOR3) and Unaffected (TOR4, TOR5) by Peat Smoldering

Profile	Horizon	Depth cm	pH	EC (dS m ⁻¹)	BD (g cm ⁻³)	DIN 19539 by SoliTOC Cube						EA	IRMS
						TOC ₄₀₀ (wt%)	ROC (wt%)	TIC (wt%)	TOC (wt%)	TC (wt%)	TN (wt%)		
TOR 1	Opov	0-14	6.8 ± 0.7	1.1 ± 0.1	0.74 ± 0.07	23.59 ± 0.22	1.03 ± 0.24	0.24 ± 0.05	24.4 ± 0.03	24.64 ± 0.07	1.56 ± 0.04	-26.7 ± 0.0	
	AB1ov	14-17	7.4 ± 0.6	4.5 ± 0.7	0.97 ± 0.09	1.10 ± 0.13	1.13 ± 0.08	0.26 ± 0.05	2.23 ± 0.05	2.49 ± 0.00	0.76 ± 0.16	-24.8 ± 0.2	
	BCov	17-30	7.9 ± 0.5	6.5 ± 0.5	0.58 ± 0.06	0.42 ± 0.02	0.32 ± 0.02	0.07 ± 0.01	0.74 ± 0.00	0.81 ± 0.00	0.17 ± 0.00	-24.6 ± 0.1	
	2BCcl	30-43	7.9 ± 0.6	2.8 ± 0.2	0.60 ± 0.05	0.05 ± 0.01	0.01 ± 0.01	0.01 ± 0.00	0.07 ± 0.02	0.07 ± 0.02	0.02 ± 0.01	-24.9 ± 0.1	
	2Ccl	43-65	7.8 ± 0.4	2.7 ± 0.3	1.01 ± 0.08	0.03 ± 0.02	0.01 ± 0.00	0.00 ± 0.00	0.05 ± 0.02	0.05 ± 0.02	0.01 ± 0.01	-23.2 ± 0.3	
TOR 2	3Oecl	65-73	5.7 ± 0.3	8.7 ± 0.9	0.88 ± 0.08	0.04 ± 0.01	0.01 ± 0.01	0.02 ± 0.01	0.06 ± 0.01	0.08 ± 0.01	0.02 ± 0.01	-25.4 ± 0.2	
	3Oipy	73-84	3.5 ± 0.3	11.7 ± 0.8	0.69 ± 0.09	8.32 ± 0.55	2.36 ± 0.46	0.08 ± 0.04	10.17 ± 0.10	10.26 ± 0.06	0.67 ± 0.09	-27.2 ± 0.2	
	4Cg	84-96+	5.9 ± 0.4	3.7 ± 0.4	1.15 ± 0.11	1.62 ± 0.08	1.07 ± 0.04	0.04 ± 0.01	2.66 ± 0.04	2.70 ± 0.04	0.23 ± 0.01	-24.5 ± 0.1	
	Opov	0-12	6.9 ± 0.7	-	0.83 ± 0.09	14.93 ± 0.54	0.96 ± 0.12	0.58 ± 0.14	15.89 ± 0.51	16.47 ± 0.36	1.33 ± 0.04	-25.7 ± 0.3	
	ACov	12-38	8.1 ± 0.5	4.7 ± 0.5	0.51 ± 0.07	0.12 ± 0.02	0.21 ± 0.03	2.83 ± 0.03	0.36 ± 0.01	3.20 ± 0.02	0.07 ± 0.01	-8.2 ± 0.0	
TOR 3	2Ckov	38-48	8.2 ± 0.5	3.0 ± 0.1	1.03 ± 0.11	0.10 ± 0.01	0.31 ± 0.03	8.87 ± 0.00	0.44 ± 0.02	9.31 ± 0.02	0.09 ± 0.02	-6.6 ± 0.2	
	3Cov	48-65	8.3 ± 0.4	3.8 ± 0.1	0.78 ± 0.04	0.18 ± 0.02	0.27 ± 0.04	0.87 ± 0.02	0.48 ± 0.06	1.34 ± 0.06	0.08 ± 0.01	-13.1 ± 0.1	
	4Oipy	65-72	4.2 ± 0.3	5.5 ± 0.3	0.71 ± 0.06	22.14 ± 0.06	0.73 ± 0.15	0.10 ± 0.01	22.90 ± 0.10	23.1 ± 0.09	1.22 ± 0.11	-26.6 ± 0.1	
	4Cg	72-90	4.9 ± 0.7	14.4 ± 0.9	1.02 ± 0.09	11.30 ± 0.18	1.03 ± 0.17	0.10 ± 0.01	12.15 ± 0.04	12.24 ± 0.04	0.64 ± 0.02	-27.0 ± 0.2	
	Opov	0-28	7.2 ± 0.1	2.4 ± 0.2	0.71 ± 0.07	17.49 ± 0.19	0.95 ± 0.08	1.22 ± 0.13	18.35 ± 0.14	19.57 ± 0.05	1.17 ± 0.04	-24.9 ± 0.0	
TOR 4	ABov	28-30	7.7 ± 0.4	2.2 ± 0.3	1.01 ± 0.11	2.66 ± 0.46	1.31 ± 0.08	0.53 ± 0.03	3.89 ± 0.43	4.42 ± 0.43	0.49 ± 0.04	-24.3 ± 0.3	
	2BCov	30-40	7.9 ± 0.6	2.1 ± 0.1	0.60 ± 0.05	0.32 ± 0.03	0.22 ± 0.03	0.54 ± 0.03	0.57 ± 0.06	1.10 ± 0.04	0.04 ± 0.01	-19.8 ± 0.1	
	2Cov	40-50	7.9 ± 0.5	2.9 ± 0.3	0.93 ± 0.09	0.27 ± 0.02	0.26 ± 0.03	0.26 ± 0.02	0.57 ± 0.05	0.83 ± 0.03	0.05 ± 0.01	-23.3 ± 0.2	
	3Oipy	50-70	5.2 ± 0.6	3.8 ± 0.4	0.70 ± 0.11	26.19 ± 0.40	0.68 ± 0.19	0.11 ± 0.00	26.86 ± 0.30	26.97 ± 0.30	1.41 ± 0.10	-26.8 ± 0.1	
	3Cg	70-90	3.3 ± 0.2	13.8 ± 0.8	1.19 ± 0.21	8.60 ± 0.10	0.63 ± 0.14	0.08 ± 0.01	9.13 ± 0.05	9.21 ± 0.04	0.51 ± 0.07	-26.6 ± 0.1	
TOR 5	Op1	0-12	7.0 ± 0.5	4.4 ± 0.3	0.76 ± 0.09	22.03 ± 0.38	0.80 ± 0.31	0.20 ± 0.03	23.08 ± 0.48	23.29 ± 0.49	1.32 ± 0.02	-26.5 ± 0.2	
	Op2	10-25	7.1 ± 0.6	4.8 ± 0.4	0.80 ± 0.07	22.19 ± 0.60	1.00 ± 0.25	0.17 ± 0.01	23.23 ± 0.57	23.40 ± 0.56	1.28 ± 0.07	-26.4 ± 0.2	
	Op3	25-38	7.0 ± 0.4	4.9 ± 0.3	0.94 ± 0.09	21.43 ± 0.64	1.19 ± 0.57	0.20 ± 0.03	22.80 ± 0.42	23.00 ± 0.40	1.26 ± 0.13	-26.1 ± 0.1	
	Oi	38-47	4.2 ± 0.2	9.0 ± 0.7	0.83 ± 0.07	23.82 ± 0.98	0.57 ± 0.16	0.10 ± 0.01	24.40 ± 0.96	24.51 ± 0.96	1.08 ± 0.22	-26.5 ± 0.0	
	Cg	47-54	3.5 ± 0.1	7.6 ± 0.4	1.09 ± 0.11	1.68 ± 0.08	0.38 ± 0.05	0.03 ± 0.00	2.00 ± 0.03	2.03 ± 0.03	0.21 ± 0.01	-27.1 ± 0.1	

Table 1
Continued

Profile	Horizon	Depth cm	pH	EC (dS m ⁻¹)	BD (g cm ⁻³)	DIN 19539 by SoliTOC Cube					EA		IRMS
						TOC ₄₀₀ (wt%)	ROC (wt%)	TIC (wt%)	TOC (wt%)	TC (wt%)	TN (wt%)	δ ¹³ C _{TC} (‰)	
	Oi	36–45	5.5 ± 0.7	7.6 ± 0.7	1.01 ± 0.10	22.15 ± 1.12	0.77 ± 0.03	0.11 ± 0.00	22.96 ± 1.14	23.07 ± 1.15	1.25 ± 0.05	-27.5 ± 0.1	
	C	45–60	3.6 ± 0.3	13.3 ± 0.1	1.27 ± 0.12	7.63 ± 0.11	0.56 ± 0.07	0.06 ± 0.01	8.27 ± 0.18	8.33 ± 0.17	0.48 ± 0.02	-26.3 ± 0.2	

Note. The reported results are the average of three analytical replicates with the relative standard deviation. Abbreviations: BD, bulk density; EA, elemental analyzer; EC, electrical conductivity; IRMS, isotope ratio mass spectrometer; n.a., not analyzed; TC, total carbon; TIC, total inorganic carbon; TN, total nitrogen.

4.2. Soil Carbon Pools on F and NF Profiles

Carbon speciation of the F and NF peat profiles was carried out in compliance with the DIN 19539 standard, where four carbon fractions were measured: TC, TOC₄₀₀, ROC, and TIC. The carbon speciation results are presented in Table 1 and Figures 3 and 4. The two-way ANOVA test showed that all the elemental and isotopic variables of F and NF samples were affected by both the profile and the depth of sampling (*p*-values < 0.0001).

TC of the NF peat profiles was determined to be generally higher than that of the F profiles.

The TC of the NF peat profiles equaled approximately 20–25 wt% from the surface down to a depth of 40 cm, diminished at the Cg and C horizons, and reached the maximum of 34 wt% in the Oi horizon of TOR4 at a depth of 54–63 cm.

The TC of the F peat profiles was comparable with that of the NF profiles in the shallow horizons (16–25 wt%, down to a depth of 15 cm) and dramatically decreased (down to 0 wt% in some cases) at variable depths between 14–73 cm (TOR1), 12–65 cm (TOR2), 28–50 cm (TOR3). Profile TOR2 presented a notable exception, where the intermediate 2Ckov horizon (38–48 cm depth) was characterized by a TC reaching 9 wt%. The TC of the F profiles increased downward, with values up to 10 wt% at 73–84 cm in TOR1, 23 wt% at 65–72 cm in TOR2, and 27 wt% at a depth of 50–70 cm in TOR3.

The distribution of TOC₄₀₀ with depth was determined to be similar to that of TC, suggesting that most carbon in the investigated peat profiles belongs to the thermally labile organic pool. In the NF profiles, TOC₄₀₀ was on average 20 wt% down to a depth of 50 cm, decreasing in the Cg and 2Cg horizons in TOR4, and in the C horizon in TOR5. The relative amount of the TOC₄₀₀ fraction (TOC₄₀₀%) was always >75% of the TC along the NF profiles.

In the F profiles, the TOC₄₀₀ values (14–24 wt%) were comparable with those of the NF profiles in the shallower horizons down to a depth of 15 cm, dramatically decreasing (approaching zero) at depths between 14–73 cm (TOR1), 12–65 cm (TOR2), and 28–50 cm (TOR3). The deeper horizons of the F profiles were characterized by a marked increase in the TOC₄₀₀ values, varying from 8.3 wt% at 73–84 cm in TOR1, to 22 wt% at 65–72 cm in TOR2, and to 26 wt% at 50–70 cm in TOR3.

The ROC content was similar in the F and NF profiles in the shallow horizons, showing values around 1 wt%. A marked ROC decrease occurred in the lower horizons of the F profiles, where ROC reached approximately 0 wt% at 30–73 cm in TOR1, 0.2–0.3 wt% at 12–65 cm in TOR2, and 0.2–0.3 wt% at 30–50 cm in TOR3, followed by a variable ROC increase with depth.

The TIC content varied from 2.8 wt% (TOR5) to 0.2 wt% (TOR2 and TOR4) in the superficial horizons and decreased with depth in both the F and NF profiles. The only exception was represented by the TOR1 profile, characterized by a TIC approaching zero in the intermediate horizons (30–73 cm depth), with a slight increase in the TIC values downward. The relative amount of TIC with respect to TC (TIC%) varied from 0% to 95%, with the highest values recorded in the intermediate horizons of the F profiles.

The bulk carbon isotopic composition (δ¹³C_{TC}) of the NF horizons varied between -27.5‰ (TOR5, Oi, 36–45 cm depth) and -21.5‰ (TOR5, Ap, 0–25 cm depth).

A marked variation was observed in the δ¹³C_{TC} of the F profiles, where δ¹³C_{TC} changed from -27.2‰ (TOR1, 30Ipy, 73–84 cm depth) to -6.6‰ (TOR2, 2Ckov, 38–48 cm depth), with less negative values recorded in the intermediate horizons (Figures 3 and 4).

A very good linear correlation between δ¹³C_{TC} and TIC% (*r*² = 0.9) confirmed that the bulk carbon isotopic value is directly related to the relative amount of a carbonate endmember.

The total nitrogen (TN) elemental content was also determined and varied from 1.56 wt% (TOR1, 0–14 cm depth) to 0.01 wt% (TOR1, 30–73 cm depth), showing a significant positive correlation with the TOC (TOC₄₀₀ + ROC) parameter.

Differences between F and NF soil profiles can be emphasized with a statistical elaboration of the available data, as shown in the PCA reported in Figure 5. The PCA is able to group the TOR profiles on the

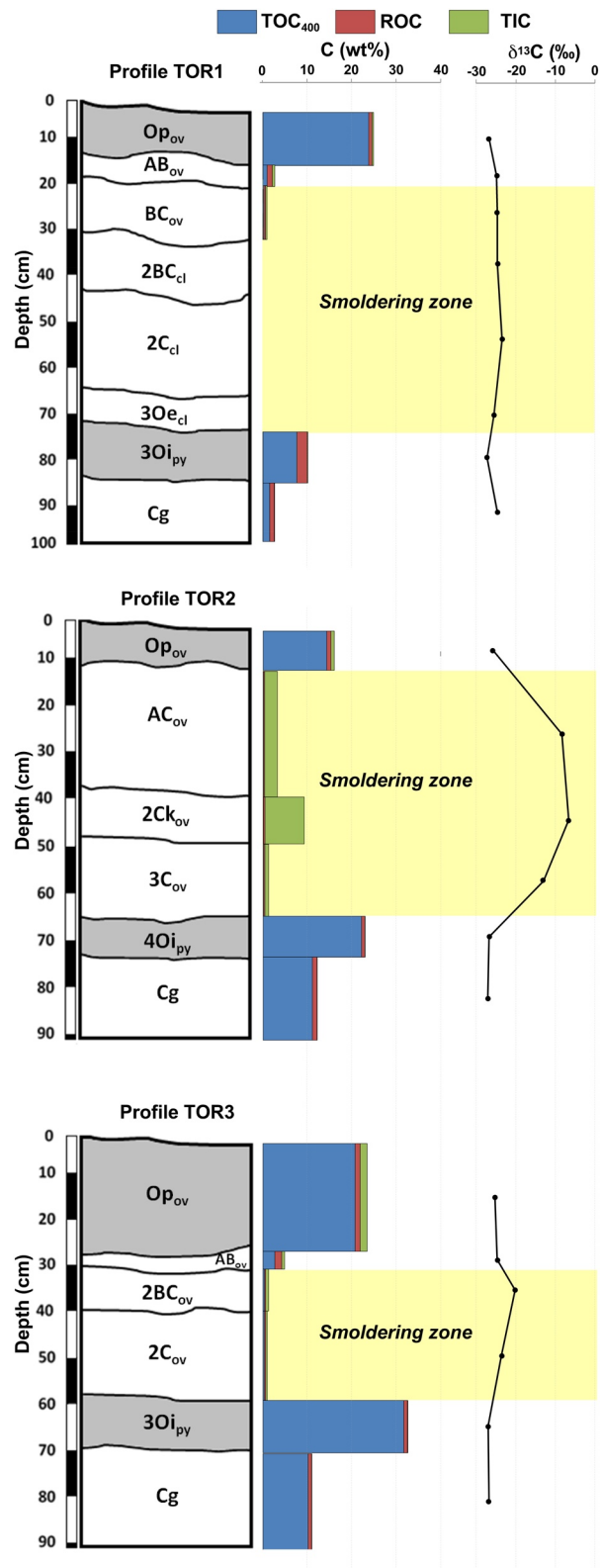


Figure 3. Carbon speciation of soil profiles variably affected by peat smoldering (TOR1, TOR2, TOR3). Histograms refer to the three soil carbon pools defined by the DIN 19539 standard (TOC₄₀₀, ROC, total inorganic carbon). The bulk carbon isotopic composition ($\delta^{13}C_{TC}$) is also reported. Note that the depth of the smoldering zone is indicated by the yellow box. See text for further details.

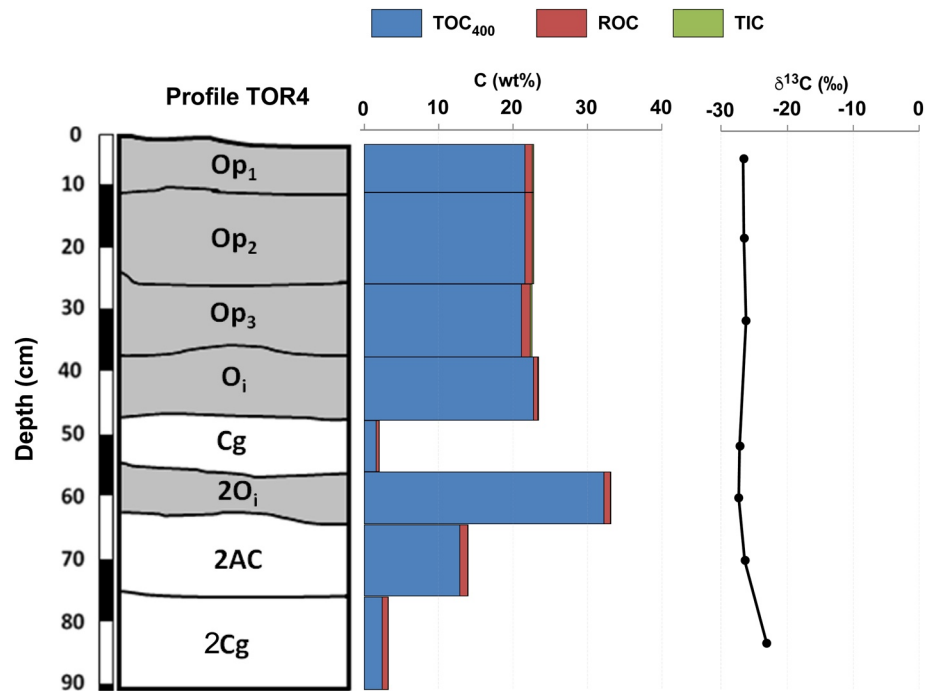


Figure 4. Carbon speciation in soil profile TOR4, taken as representative soil profile unaffected by peat smoldering. Histograms refer to the three soil carbon pools defined by the DIN 19539 standard (TOC₄₀₀, ROC, total inorganic carbon). The bulk carbon isotopic composition ($\delta^{13}\text{C}_{\text{TC}}$) is also reported.

basis of many variables called principal components, which can describe correlations among the studied samples. We considered the TOC₄₀₀, ROC, TC, TIC, N and $\delta^{13}\text{C}$ as principal components and we focused the statistical analyses on horizons ranging from 30 to 70 cm where smoldering was effective. Noteworthy, the first and second PCA axes explained 74.6% and 20.3% of the variance, respectively. In the plot the NF profiles showed a clear grouping, which was driven by high content of organic carbon fractions (TOC₄₀₀, ROC, and TOC) and N. On the other hand, F profiles plot in opposite areas of the PCA diagram, reflecting lower content of organic carbon fractions and N.

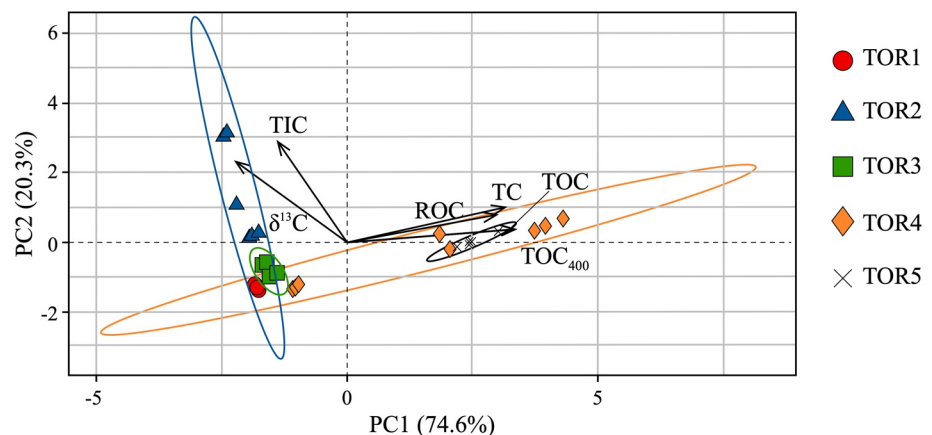


Figure 5. Principal component analysis of F and NF soil profiles.

Table 2
Carbon Fractions (and Isotope Composition) and Nitrogen of the Experimentally Fired Horizons From Soil Profile TOR4

Profile	Horizon	Depth cm	T treatment (°C)	DIN19539	by SoliTOC Cube		TOC (wt%)	TC (wt%)	EA	IRMS
				TOC ₄₀₀ (wt%)	ROC (wt%)	TIC (wt%)			TN (wt%)	$\delta^{13}\text{C}_{\text{TC exp}}$ (‰)
TOR4	Op3	25–38	105	21.83 ± 0.92	0.70 ± 0.01	0.19 ± 0.03	22.53 ± 0.91	22.73 ± 0.94	1.20 ± 0.01	-25.9 ± 0.1
			200	21.01 ± 0.44	1.39 ± 0.51	0.21 ± 0.02	22.40 ± 0.06	22.62 ± 0.06	1.30 ± 0.08	-25.6 ± 0.1
			400	0.56 ± 0.16	1.39 ± 0.14	0.26 ± 0.02	1.94 ± 0.02	2.21 ± 0.03	0.30 ± 0.00	-21.4 ± 0.2
			600	0.14 ± 0.08	0.24 ± 0.12	0.15 ± 0.02	0.40 ± 0.17	0.55 ± 0.15	0.02 ± 0.00	-17.5 ± 0.3
TOR4	Cg	47–54	105	2.09 ± 0.10	0.37 ± 0.03	0.03 ± 0.00	2.46 ± 0.08	2.49 ± 0.08	0.22 ± 0.03	-27.0 ± 0.2
			200	1.83 ± 0.08	0.42 ± 0.03	0.03 ± 0.00	2.26 ± 0.10	2.28 ± 0.10	0.23 ± 0.02	-27.0 ± 0.0
			400	0.09 ± 0.00	0.18 ± 0.03	0.03 ± 0.00	0.27 ± 0.00	0.30 ± 0.00	0.12 ± 0.01	-26.1 ± 0.2
			600	0.04 ± 0.02	0.02 ± 0.02	0.01 ± 0.00	0.08 ± 0.01	0.08 ± 0.01	0.01 ± 0.01	-26.6 ± 0.1
TOR4	2AC	63–75	105	11.03 ± 0.69	0.44 ± 0.15	0.06 ± 0.01	11.47 ± 0.58	11.54 ± 0.58	0.53 ± 0.01	-26.2 ± 0.1
			200	5.99 ± 0.09	0.73 ± 0.15	0.04 ± 0.00	6.73 ± 0.20	6.76 ± 0.20	0.45 ± 0.02	-26.0 ± 0.1
			400	0.08 ± 0.02	0.25 ± 0.02	0.04 ± 0.00	0.33 ± 0.00	0.37 ± 0.00	0.13 ± 0.00	-24.7 ± 0.3
			600	0.04 ± 0.03	0.01 ± 0.00	0.01 ± 0.00	0.06 ± 0.01	0.08 ± 0.01	0.02 ± 0.01	-26.5 ± 0.3
TOR4	2Cg	75–5+	105	1.96 ± 0.00	1.30 ± 0.08	0.04 ± 0.00	3.27 ± 0.08	3.31 ± 0.09	0.24 ± 0.01	-21.4 ± 0.3
			200	2.01 ± 0.03	1.11 ± 0.15	0.04 ± 0.00	3.12 ± 0.17	3.16 ± 0.17	0.26 ± 0.01	-21.2 ± 0.4
			400	0.14 ± 0.00	0.59 ± 0.03	0.05 ± 0.01	0.74 ± 0.03	0.79 ± 0.03	0.12 ± 0.01	n.a.
			600	0.06 ± 0.04	0.02 ± 0.01	0.02 ± 0.00	0.10 ± 0.01	0.11 ± 0.01	0.02 ± 0.00	-21.5 ± 0.3

Abbreviations: EA, elemental analyzer; IRMS, isotope ratio mass spectrometer; n.a., not analyzed; TC, total carbon; TIC, total inorganic carbon; TN, total nitrogen.

4.3. Soil Carbon Pools of the Experimentally Fired Profiles

The results of carbon speciation of the experimentally fired soil horizons from the NF profile (TOR4) are presented in Table 2 and Figure 6.

TC varied insignificantly in the samples heated to 200°C, except for horizon 2AC, where the TC content was reduced by 40% between 105°C and 200°C. A remarkable TC decrease was recorded in the samples heated to 400°C, and very little carbon was left in the samples after heating them to 600°C. The TC decrease with the increasing temperature was irrespective of the TC content in the untreated samples.

Regarding the carbon fractions, TOC₄₀₀ was the most abundant, and its relative contribution in the untreated samples varied from 93% (Op3) to approximately 75% (2Cg). TOC₄₀₀ did not exhibit any remarkable variation in the samples heated to 200°C, whereas it generally disappeared when the temperatures reached 400°C.

The relative contribution of ROC with respect to TC varied from approximately 5% (Op3) to 26% (2Cg) in the untreated samples. The behavior of ROC in response to thermal treatment was similar to that of TOC₄₀₀ in the samples heated to 200°C. A slight non-systematic variation of ROC was recorded in the samples heated to 400°C, and ROC disappeared when the temperature reached 600°C.

The TIC content remained nearly constant during all heating treatments for all samples and was best represented in the Op3 horizon, where it constituted 0.20 wt% and 0.15 wt% in the untreated and treated (heated to 600°C) samples, respectively.

The relative amount of inorganic carbon with respect to TC (TIC%) increased with increasing temperature, and the highest variations were recorded in the samples heated to 400°C and 600°C when the two organic fractions were exhausted. TIC% was less than 1% in the untreated samples and up to 26% in the samples heated to 600°C.

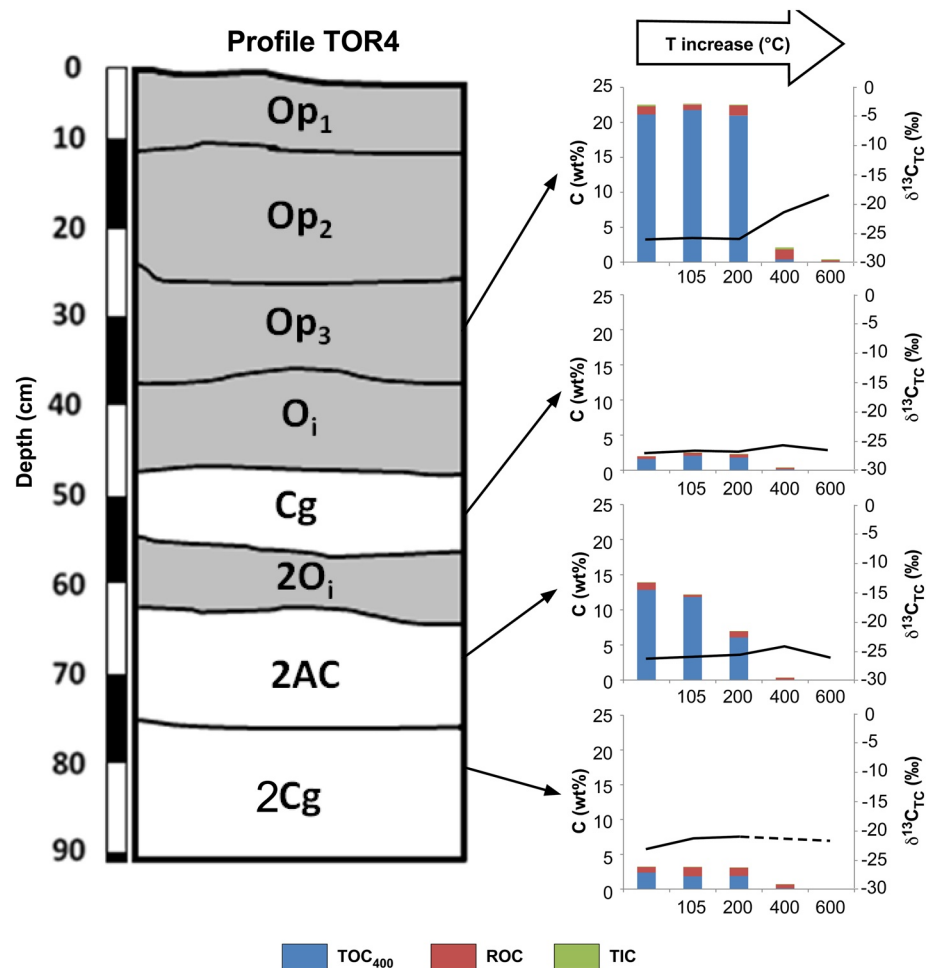


Figure 6. Carbon speciation of experimentally fired horizons from soil profile TOR4. Histograms refer to the three soil carbon pools defined by the DIN19539 standard (TOC₄₀₀, ROC, total inorganic carbon). The bulk carbon isotopic composition ($\delta^{13}\text{C}_{\text{TCexp}}$) is also reported.

The carbon isotopic composition ($\delta^{13}\text{C}_{\text{TCexp}}$) was less negative when the temperature increased. The greatest variation was recorded in the Op3 horizon, where $\delta^{13}\text{C}_{\text{TCexp}}$ were -26.1‰ and -17.5‰ in the untreated and treated (heated to 600°C) samples, respectively. This variation is likely related to the loss of TOC₄₀₀ and increased TIC contribution to TC when the temperature escalated.

5. Discussion

5.1. Effects of Soil Burning in the Mezzano Lowland

The significant differences recorded in the physicochemical characteristics of the F and NF peaty soil profiles give insights on the magnitude of fire events in terms of their temperature, depth, and loss of carbon stock. The opposite trend of pH variation at depths of 14–73 cm (TOR1), 12–65 cm (TOR2), and 28–50 cm (TOR3) of the F with respect to the NF (TOR4 and TOR5) soil profiles suggests that burning modified the ML peaty soils at depth. The observed increase in pH in the F profiles at the intermediate depths mentioned above is consistent with the destabilization of organic acids and the enhanced contribution of carbonates and oxides, as a consequence of firing events (Granged et al., 2011a, 2011b; Kutiel et al., 1990; Ulery et al., 1995). The observed variation (3–4 pH units) in the F profiles suggests that they underwent high fire intensity (Ulery et al., 1995). The F profile horizons are also characterized by lower EC values compared with those of the NF profiles in the aforementioned depth intervals, likely due to the destruction of clay minerals and the formation of oxides at temperatures exceeding 500°C (Terefe et al., 2008). Low BD values

(0.60–0.51 g cm⁻³) noted in some horizons of the TOR1, TOR2, and TOR3 profiles can be ascribed to “unpacking” of particles (Ngole-Jeme, 2019) resulting from the loss of structure due to degradation of mineral and organic components.

The temperature to which the F profiles were exposed can be estimated by analyzing carbon fractions with different thermal stabilities. The thermally labile fraction (TOC₄₀₀) is always present in the superficial horizons of the F profiles, with average relative amounts (TOC_{400%}) of 90%, and is comparable to that observed in the NF profiles. The marked decrease in the TOC₄₀₀ fraction with depth (until it disappears) indicates that the F soil profiles were heated to over 400°C at depths of 14–73 cm (TOR1), 12–65 cm (TOR2), and 28–50 cm (TOR3) (Figure 3). The soil color change from dark brown (in the upper and lower horizons) to reddish at the intermediate depths also supports this finding, indicating burning temperatures of 300°C–500°C (Terefe et al., 2005, 2008). A sudden increase in the TOC₄₀₀ fraction at greater depths in the F soil profiles suggests a sharp decrease in the firing temperature downward.

The distribution of ROC along the F soil profiles is more variable. Only TOR1 records the total exhaustion of ROC at depths of 30–73 cm, whereas TOR2 and TOR3 show a significant decrease in the ROC content (down to 0.2 wt%) at depths of 12–65 and 30–50 cm, respectively. Such ROC content distribution indicates that the firing temperature exceeded 600°C only in TOR1, whereas TOR2 and TOR3 were subjected to maximum temperatures of 400–600°C. These observations provide new insights into the thermal persistence of SOM, which was previously thought to disappear at temperatures of 450–500°C (Knoepp et al., 2005). The TIC fraction gradually decreases with depth in the F and NF profiles. The total exhaustion of TIC was only recorded in profile TOR1 at depths of 30–73 cm, suggesting that the layer was subjected to the maximum temperature (potentially exceeding 750°C) during the fire event. The significant correlation of TN with TOC₄₀₀ (and not with ROC) indicates that nitrogen is mostly volatilized at relatively low temperatures ($T < 400^{\circ}\text{C}$) during firing events, as already reported in the literature (Turner et al., 2007). Moreover, the ubiquitous persistence of high TOC₄₀₀ and TN values in the superficial layers of the F profiles indicates that smoldering generally started and developed with variable intensity between depths of 10 and 70 cm.

Both the organic-rich (Op3) and organic-poor (Cg) horizons present similar thermal behavior of their carbon fractions. The total disappearance of the TOC₄₀₀ fraction (and TN) at heating temperatures over 400°C makes this fraction a robust thermal marker for the investigated profiles. Analogous conclusions can be made for the ROC fraction, which indicates heating temperatures below 600°C. The TIC fraction varied little in the experimental heating interval, and its presence in profiles TOR2 and TOR3 mainly implies that they did not undergo carbonate destabilization, which should occur at a temperature of approximately 750°C.

The bulk carbon isotopic composition of the experimentally heated NF horizons becomes less negative with increasing temperatures. This trend is similarly observed in the natural F profiles but does not imply the neof ormation of carbonates during firing. The least negative values recorded in profile TOR2 at depths of 12–65 cm likely reflect the concentration of soil carbonates originally present in this horizon.

5.2. Triggering Mechanisms of Soil Burning in the Mezzano Lowland

Peat burning in the ML is not induced by surface flaming with downward propagation, as it is triggered at depth and develops in the 10–70 cm-deep soil horizons via smoldering combustion. This evidence suggests self-combustion of the organic-rich soils. Similar processes have been described in the literature, especially in dry and warm conditions (Restuccia et al., 2017), and are explained as the result of multiple reaction steps including drying, biological activity, and oxidation, that are necessary to trigger the the spontaneous ignition of peat-soils (Yuan et al., 2021).

In the present case-study we suggest that the exothermal oxidation of methane (Christophersen et al., 2001; Pehme et al., 2020), which in the ML typically rises from the deep stratigraphic layers, plays an additional role either in triggering the peat smoldering. The hypothesis is based on the fact that peat smoldering in the area is spatially associated to localized sectors characterized by high CH₄ seepage (with fluxes up to 120 g m⁻² day⁻¹, according to Cremonini et al., 2008). Soil heating occurs at depth where there is the transition between anoxic and oxic conditions with concomitant methanotrophic bacteria activity that promotes

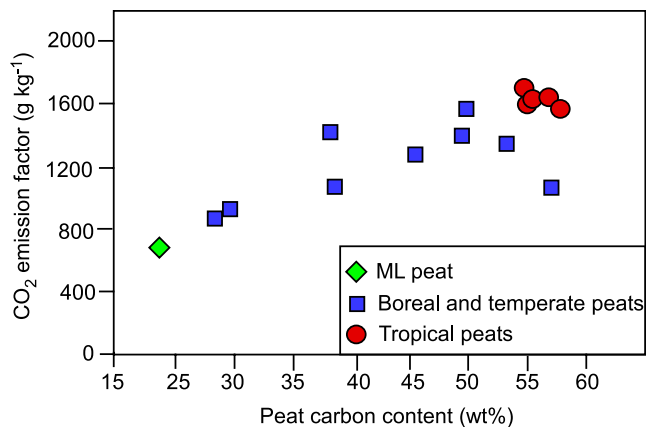


Figure 7. CO₂ emission of burning Mezzano Lowland peat-soils, compared with that of burning peat-soils from other areas.

temperature well exceeding 40°C (Capaccioni et al., 2015), which is considered a thermal condition necessary for self-heating propensity (Yuan et al., 2021).

In this light, a possible strategy to minimize the peat-smoldering occurrence would require (a) the controlled collection of the uprising methane and (b) to maximize the irrigation efficiency of the area, that should be specifically planned to convey water at the soil depths where smoldering is effective.

5.3. Environmental Consequences of Peat Burning in the Mezzano Lowland

Peat burning implies environmental consequences in terms of release of greenhouse gases (Kohlenberg et al., 2018; Prosperi et al., 2020). The data described above allow the calculation of the soil organic carbon (SOC) stock in the F and NF profiles, and in turn the SOC stock is useful for estimating losses caused by burning events. The NF profile of TOR4 has a SOC stock of approximately 150 kg m⁻² for a thickness of 90 cm. These values are representative for ML soils unaffected by peat burning, as highlighted by the analyses of other soil profiles from the surroundings (see Table S2). A decrease in the SOC stock is observed in profiles TOR3 and TOR2 and, especially, in TOR1, characterized by the lowest SOC stock 38 kg m⁻² for a thickness of 96 cm. We infer that peat fires in the ML degraded up to two-thirds of the previous SOC stock. Although the extent of peat fire events is variable, we estimate that an average loss of the SOC stock within the first meter of depth is approximately 110 kg m⁻², potentially corresponding to approximately 580 kg CO₂ m⁻³ of emissions. As reported in Figure 7, the resulting emission coefficient is 725 g of CO₂ for kg of smoldered soil, a value that is compatible with what observed in other study-cases of smoldering peat soils in temperate climatic settings. However, carbon emissions plausibly include a wide spectrum of distinct components, where CO₂ is accompanied by CO, volatile organic components as well as by particulate matter (PM) having micrometer and sub-micrometer size range (Hu et al., 2018).

5.4. Impacts of Peat Burning on the Human Health

The peat burning generates long-term smoke which is released in the air (Figure 2d). These emissions are mainly composed by carbon monoxide, carbon dioxide, nitrate and sulfate, which are hazardous volatiles for the human health and if inhaled can trigger several symptoms from throat irritation, cough, and headaches to serious respiratory and cardiovascular problems, especially for people with existing asthma, emphysema, and heart disease (Hinwood & Rodriguez, 2005; Hu et al., 2018; Rappold et al., 2011).

Besides volatiles, the peat burning releases fine particles such as PM₁₀ and/or PM_{2.5} depending on the predominance of coarse (particle diameter < 10 μm) or fine (particles diameter < 2.5 μm) soil fractions (Hinwood & Rodriguez, 2005). If inhaled PM₁₀ and PM_{2.5} cause damages of lung tissue and respiratory and cardiovascular problems (Hu et al., 2018). The potential health risk of the smoke is even more serious considering the duration of the peat burning, as the prolonged or repeated smoke and particulate exposure by local people may aggravate the adverse health outcomes causing long-term health effects.

Additional concerns are related to elements potentially toxic (e.g., several heavy metals such as Co, Cr, Cu, Ni, V, Zn, Pb, As, Mo, Se, Cd, Mo) that in the studied soils appear bounded in organo-metallic compounds (Di Giuseppe et al., 2014b, 2014c), because they could be released in the environment, in concomitance with the SOM destabilization, contaminating air, aquifers and soils (Kohlenberg et al., 2018).

In our view, the volatilization in the atmosphere or the dissolution in the hydrosphere of elements critical for the human health deserve further research on the peat-burning processes occurring in the Mezzano Lowland. In addition, the designed authorities should inform and educate locals about the health-risk of the peat smoke exposure.

6. Conclusions

Peat fires variously affect the first meter of soil profiles in the ML, and their intensity can be evaluated recording the differential consumption of the carbon pools with distinct thermal stabilities. The main damage to soil carbon budget occurs in the 10–70 cm-deep horizons, where smoldering temperatures of 400–600°C cause the total exhaustion of TOC₄₀₀ and variably decrease the ROC contents. Evidence of extreme temperatures overcoming the destabilization of carbonates ($\geq 750^\circ\text{C}$) is limited to the inner horizons of the smoldering zone. The process appears spontaneous and shows analogies with what observed in other case-studies where peat self-combustion requires multiple reaction steps (drying, biological activity, and oxidative oxidation), but in the ML is possibly facilitated by the concomitant upraising of deep methane and its exothermal oxidation. The estimated carbon emission is 110 kg m^{-2} , corresponding to $580 \text{ kg CO}_2 \text{ m}^{-3}$, values in the same order of magnitude estimated in other temperate areas affected by smoldering peat-soils. The consequent release of significant amounts of greenhouse gases is coupled with a loss of soil structure, nutrients (e.g., nitrogen), and possibly also toxic elements (e.g., heavy metals). The consequences are surely negative for the environment, the agricultural activities and plausibly also for the health of the local people, and deserve further investigation to plan mitigation strategies for ongoing and future smoldering episodes.

Conflict of Interest

The authors declare no conflicts of interest relevant to this study.

Data Availability Statement

Data supporting our conclusions can be obtained from the Open Science Framework website at <https://osf.io/vq7fu/> (<https://doi.org/10.17605/OSF.IO/VQ7FU>)

Acknowledgment

This study was supported by the European Agricultural Fund for Rural Development (project SaveSOC2, ID: 2017IT06RDEI5015638 v1), allocated by the Emilia-Romagna region (PSR 2014-2020).

References

- Abram, N. J., Henley, B. J., Gupta, A. S., Lippmann, T. J. R., Clarke, H., Dowdy, A. J., et al. (2021). Connections of climate change and variability to large and extreme forest fires in southeast Australia. *Communications Earth & Environment*, 2, 8. <https://doi.org/10.1038/s43247-020-00065-8>
- Amorosi, A., Centineo, M. C., Dinelli, E., Lucchini, F., & Tateo, F. (2002). Geochemical and mineralogical variations as indicators of provenance changes in Late Quaternary deposits of SE Po Plain. *Sedimentary Geology*, 151, 273–292. [https://doi.org/10.1016/S0037-0738\(01\)00261-5](https://doi.org/10.1016/S0037-0738(01)00261-5)
- Beccaluva, L., Bianchini, G., Natali, C., & Siena, F. (2017). The alkaline–carbonatite complex of Jacupiranga (Brazil): Magma genesis and mode of emplacement. *Gondwana Research*, 44, 157–177. <https://doi.org/10.1016/j.jgr.2016.11.010>
- Belyea, L. R., & Malmer, N. (2004). Carbon sequestration in peatland: Patterns and mechanisms of response to climate. *Global Change Biology*, 10, 1043–1052. <https://doi.org/10.1111/j.1529-8817.2003.00783.x>
- Bianchini, G., Di Giuseppe, D., Natali, C., & Beccaluva, L. (2013). Ophiolite inheritance in the Po plain sediments: Insights on heavy metals distribution and risk assessment. *Ofioliti*, 38, 1–14. <https://doi.org/10.4454/ofioliti.v38i1.414>
- Bianchini, G., Laviano, R., Lovo, S., & Vaccaro, C. (2002). Chemical-mineralogical characterisation of clay sediments around Ferrara (Italy): A tool for an environmental analysis. *Applied Clay Science*, 21, 165–176. [https://doi.org/10.1016/S0169-1317\(01\)00086-2](https://doi.org/10.1016/S0169-1317(01)00086-2)
- Bianchini, G., Natali, C., Di Giuseppe, D., & Beccaluva, L. (2012). Heavy metals in soils and sedimentary deposits of the Padanian Plain (Ferrara, Northern Italy): Characterisation and biomonitoring. *Journal of Soils and Sediments*, 12, 1145–1153. <https://doi.org/10.1007/s11368-012-0538-5>
- Boehm, H.-D. V., Siegert, F., Riele, J. O., Page, S. E., Jauhainen, J., Vasanser, H., & Jaya, A. (2001). Fire impacts and carbon release on tropical peatlands in Central Kalimantan, Indonesia. In *Proceedings of the 22nd Asian Conference on Remote Sensing*, 5–9 November 2001, Singapore.
- Bonzi, L., Ferrari, V., Martinelli, G., Norelli, E., & Severi, P. (2017). Unusual geological phenomena in the Emilia-Romagna plain (Italy): Gas emissions from wells and the ground, hot water wells, geomorphological variations A review and an update of documented reports. *Bollettino di Geofisica Teorica ed Applicata*, 58, 87–102. <https://doi.org/10.4430/bgta0193>
- Capaccioni, B., Tassi, F., Cremonini, S., Sciarra, A., & Vaselli, O. (2015). Ground heating and methane oxidation processes at shallow depth in Terre Calde di Medolla (Italy): Observations and conceptual model. *Journal of Geophysical Research: Solid Earth*, 120, 3048–3064. <https://doi.org/10.1002/2014JB011635>
- Christophersen, M., Kjeldsen, P., Helle Holst, H., & Chanton, J. (2001). Lateral gas transport in soil adjacent to an old landfill: Factors governing emissions and methane oxidation. *Waste Management & Research*, 19, 595–612. <https://doi.org/10.1177/0734242X0101900616>
- Cremonini, S., Etioppe, G., Italiano, F., & Martinelli, G. (2008). Evidence of possible enhanced peat burning by deep-origin methane in the Po River delta plain (Italy). *The Journal of Geology*, 116, 401–413. <https://doi.org/10.1086/588835>
- Di Giuseppe, D., Bianchini, G., Faccini, B., & Coltorti, M. (2014a). Combination of WDXRF analysis and multivariate statistic for alluvial soils classification: A case study from the Padanian Plain (Northern Italy). *X-Ray Spectrometry*, 43, 165–174. <https://doi.org/10.1002/xrs.2535>

- Di Giuseppe, D., Bianchini, G., Vittori Antisari, L., Martucci, A., Natali, C., & Beccaluva, L. (2014b). Geochemical characterization and biomonitoring of reclaimed soils in the Po River Delta (Northern Italy): Implications for the agricultural activities. *Environmental Monitoring and Assessment*, *186*, 2925–2940. <https://doi.org/10.1007/s10661-013-3590-8>
- Di Giuseppe, D., Vittori Antisari, L., Ferronato, C., & Bianchini, G. (2014c). New insights on mobility and bioavailability of heavy metals in soils of the Padanian alluvial plain (Ferrara Province, northern Italy). *Chemie der Erde*, *74*, 615–623. <https://doi.org/10.1016/j.chemer.2014.02.004>
- Dutta, K., Schuur, E. A. G., Neff, J. C., & Zimov, S. A. (2006). Potential carbon release from permafrost soils of Northeastern Siberia. *Global Change Biology*, *12*, 1–2351. <https://doi.org/10.1111/j.1365-2486.2006.01259.x>
- Garzanti, E., Resentini, A., Vezzol, G., Andò, S., Malusà, M., & Padoan, M. (2012). Forward compositional modelling of Alpine orogenic sediments. *Sedimentary Geology*, *28*, 149–164. <https://doi.org/10.1016/j.sedgeo.2012.03.012>
- Gonfiantini, R., Stichler, W., & Rozanski, K. (1995). Standards and intercomparison materials distributed by the International Atomic Energy Agency for stable isotope measurements. In W., Stichler (Ed.), *Reference and Intercomparison Materials for Stable Isotopes of Light Elements* (pp. 13–29). Vienna. IAEA.
- Gonzalez-Vila, F. J., & Galmendros (2003). Thermal transformation of soil organic matter by natural fires and laboratory-controlled heatings. In R. Ikan (Ed.), *Natural and laboratory-simulated thermal geochemical processes* (pp. 153–200). Dordrecht. Springer. https://doi.org/10.1007/978-94-017-0111-2_4
- Granged, A. J. P., Jordán, A., Zavala, L. M., Muñoz-Rojas, M., & Mataix-Solera, J. (2011a). Short-term effects of experimental fires for a soil under eucalyptus forest (SE Australia). *Geoderma*, *167–168*, 125–134. <https://doi.org/10.1016/j.geoderma.2011.09.011>
- Granged, A. J. P., Zaval, L. M., Jordán, A., & Barcnas-Moreno, G. (2011b). Post-fire evolution of soil properties and vegetation cover in a Mediterranean heathland after experimental burning: A 3-year study. *Geoderma*, *164*, 85–94. <https://doi.org/10.1016/j.geoderma.2011.05.017>
- Hinwood, A. L., & Rodriguez, C. M. (2005). Potential health impacts associated with peat smoke: A review. *Journal of the Royal Society of Western Australia*, *88*, 133–138.
- Hu, Y., Fernandez-Anez, N., Smith, T. E. L., & Rein, G. (2018). Review of emissions from smouldering peat fires and their contribution to regional haze episodes. *International Journal of Wildland Fire*, *27*, 293–312. <https://doi.org/10.1071/WF17084>
- IPCC (2007). Climate change (2007). In S. Solomon, D. Qin, M. Manning, Z. Chen, M. Marquis, K. B. Averyt, et al. (Eds.), *The physical science basis contribution of working group I to the fourth assessment report of the intergovernmental panel on climate change*, Cambridge University Press, Cambridge, 996 pp.
- Joosten, H., & Clarke, D. (2002). Wise use of mires and peatlands. International Mire Conservation Group/International Peat Society, Saarijärvi, Finland, 253 pp.
- Kassambara, F. M. (2017). factoextra: Extract and visualize the results of multivariate data analyses. R package version 1.0.7. Retrieved from <https://CRAN.R-project.org/package=factoextra>
- Knoepp, J. D., Deban, L. F., & Neary, D. G. (2005). Soil chemistry. In D. G. Neary, K. C. Ryan, & L. F. Deban (Eds.), *Wildland fire in Ecosystems: Effects of fire on soil and water*. U.S.D.A. Forest Service General Technical Reports RMRS-GTR-42 (Vol. 4, pp. 53–71). Ogden, UT.
- Kohlenberg, A. J., Turetsky, M. R., Thompson, D. K., Branfireun, B. A., & Mitchell, C. P. J. (2018). Controls on boreal peat combustion and resulting emissions of carbon and mercury. *Environmental Research Letters*, *13*, 035005. <https://doi.org/10.1088/1748-9326/aa9ea8>
- Kreye, J. K., Varner, J. M., & Knapp, E. E. (2011). Effects of particle fracturing and moisture content on fire behavior in masticated fuelbeds burning in a laboratory. *International Journal of Wildland Fire*, *20*, 308–317. <https://doi.org/10.1071/WF09126>
- Kusaka, S., & Nakano, T. (2014). Carbon and oxygen isotope ratios and their temperature dependence in carbonate and tooth enamel using GasBench II preparation device. *Rapid Communications in Mass Spectrometry*, *28*, 563–567. <https://doi.org/10.1002/rcm.6799>
- Kutiel, P., Naveh, Z., & Kutiel, H. (1990). The effect of a wildfire on soil nutrients and vegetation in an Aleppo pine forest on Mount Carmel, Israel. In J. G. Goldammer & M. J. Jenkins (Eds.), *Fire in ecosystem dynamics: Mediterranean and northern perspectives* (pp. 85–94). The Hague, The Netherlands. SPB Academic Publishing.
- Langmann, B., & Heil, A. (2004). Release and dispersion of vegetation and peat fire emissions in the atmosphere over Indonesia 1997/1998. *Atmospheric Chemistry and Physics*, *4*, 2145–2160. <https://doi.org/10.5194/acp-4-2145-2004>
- Le, S., Josse, J., & Husson, F. F. M. R. (2008). An R package for multivariate analysis. *Journal of Statistical Software*, *25*, 1–18. <https://doi.org/10.18637/jss.v025.i01>
- Marchina, C., Natali, C., & Bianchini, G. (2019). The Po River water isotopes during the drought condition of the year 2017. *Water*, *11–150*, 1–13. <https://doi.org/10.3390/w11010150>
- Marchina, C., Natali, C., Fazzini, M., Fusetti, M., Tassinari, R., & Bianchini, G. (2017). Extremely dry and warm conditions in northern Italy during the year 2015: Effects on the Po river water. *Rendiconti Lincei, Scienze Fisiche e Naturali*, *28*, 281–290. <https://doi.org/10.1007/s12210-017-0596-0>
- Martinelli, G., Cremonini, S., Samonati, E., & Stracher, G. B. (2015). Italian Peat and Coal fires. In G. B. Stracher, A. Prakash, & G. Rein (Eds.), *Coal and Peat Fires: A Global perspective*, Vol 4: Peat-geology combustion and case studies, Elsevier, Amsterdam, pp 40–73. <https://doi.org/10.1016/B978-0-444-59510-2.00003-3>
- Miola, A., Bondesan, A., Corain, L., Favaretto, S., Mozzi, P., Piovani, S., & Sostizzo, I. (2006). Wetlands in the Venetian Po Plain (north-eastern Italy) during the Last Glacial Maximum: Vegetation, hydrology, sedimentary environments. *Review of Palaeobotany and Palynology*, *141*, 53–81. <https://doi.org/10.1016/j.revpalbo.2006.03.016>
- Monroe, M. C., Watts, A. C., & Kobziar, L. N. (2009). Where there's fire, there's smoke: Air quality and prescribed burning in Florida Gainesville. University of Florida, Florida Cooperative Extension Service, Fact Sheet FOR62, 5 pp.
- Mörchen, R., Lehdorff, E., Arenas Diaz, F., Moradi, G., Bol, R., Fuentes, B., et al. (2019). Carbon accrual in the Atacama Desert. *Global and Planetary Change*, *181*, 102993. <https://doi.org/10.1016/j.gloplacha.2019.102993>
- Moreno, L., Jiménez, M.-E., Aguilera, H., Jiménez, P., & de la Losa, A. (2011). The 2009 Smouldering Peat Fire in Las Tablas de Daimiel National Park (Spain). *Fire Technology*, *47*, 519–538. <https://doi.org/10.1007/s10694-010-0172-y>
- Natali, C., Bianchini, G., & Carlino, P. (2020). Thermal stability of soil carbon pools: Inferences on soil nature and evolution. *Thermochimica Acta*, *683*, 178478. <https://doi.org/10.1016/j.tca.2019.178478>
- Natali, C., Bianchini, G., & Vittori Antisari, L. (2018). Thermal separation coupled with elemental and isotopic analysis: A method for soil carbon characterization. *Catena*, *164*, 150–157. <https://doi.org/10.1016/j.catena.2018.02.022>
- Natali, C., Bianchini, G., Vittori Antisari, L., Natale, M., & Tessari, U. (2018). Carbon and nitrogen pools in Padanian soils (Italy): Origin and dynamics of soil organic matter. *Chemie der Erde/Geochemistry*, *78*, 490–499. <https://doi.org/10.1016/j.chemer.2018.09.001>
- Ngole-Jeme, V. M. (2019). Fire-induced changes in soil and implications on soil sorption capacity and remediation methods. *Applied Sciences*, *9*, 3447. <https://doi.org/10.3390/app9173447>

- Page, S., Siegert, F., Rieley, J., Boehm, H., Jaya, A., & Limi, S. (2002). The amount of carbon released from peat and forest fires in Indonesia during 1997. *Nature*, *420*, 61–65. <https://doi.org/10.1038/nature01131>
- Pehme, K.-M., Orupöld, K., Kuusemets, V., Tamm, O., Jani, Y., Tamm, T., & Kriipsalu, M. (2020). Field study on the efficiency of a methane degradation layer composed of fine fraction soil from landfill mining. *Sustainability*, *12*, 6209. <https://doi.org/10.3390/su12156209>
- Prosperi, P., Bloise, M., Tubiello, F. N., Conchedda, G., Rossi, S., Boschetti, L., et al. (2020). New estimates of greenhouse gas emissions from biomass burning and peat fires using MODIS Collection 6 burned areas. *Climatic Change*, *161*, 415–432. <https://doi.org/10.1007/s10584-020-02654-0>
- Rappold, A. G., Stone, S. L., Cascio, W. E., Neas, L. M., Kilaru, V. J., Carraway, M. S., et al. (2011). Peat bog wildfire smoke exposure in rural North Carolina is associated with cardiopulmonary emergency department visits assessed through syndromic surveillance. *Environmental Health Perspectives*, *119*, 1415–1420. <https://doi.org/10.1289/ehp.1003206>
- R Core Team. (2017). R: A language and environment for statistical computing. (accessed on 22 June 2020). Retrieved from <https://www.R-project.org/>
- Rein, G. (2009). Smouldering combustion phenomena in science and technology. *International Review of Chemical Engineering*, *1*, 3–18.
- Rein, G. (2015). Smoldering-peat megafires: The largest fires on Earth. In B. Glenn, G. B. Stracher, A. Anupma Prakash, & G. Guillermo Rein (Eds.), *Coal and peat fires: A global perspective* (pp. 1–11). Elsevier. <https://doi.org/10.1016/B978-0-444-59510-2.00001-X>
- Rein, G., Cleaver, N., Ashton, C., Pironi, P., & Torero, J. L. (2008). The severity of smouldering peat fires and damage to the forest soil. *Catena*, *74*, 304–309. <https://doi.org/10.1016/j.catena.2008.05.008>
- Restuccia, F., Huang, X., & Rein, G. (2017). Self-ignition of natural fuels: Can wildfires of carbon-rich soil start by self-heating? *Fire Safety Journal*, *91*, 828–834. <https://doi.org/10.1016/j.firesaf.2017.03.052>
- Santos, V., & Clayton, R. N. (1995). Variations of oxygen and carbon isotopes in carbonatites: A study of Brazilian alkaline complexes. *Geochimica et Cosmochimica Acta*, *59*, 1339–1352. [https://doi.org/10.1016/0016-7037\(95\)00048-5](https://doi.org/10.1016/0016-7037(95)00048-5)
- Schoeneberger, P. J., Wysocki, D. A., Benham, E. C., & Soil Survey Staff. (2012). Field book for describing and sampling soils, version 3.0. Natural Resources Conservation Service, National Soil Survey Center, Lincoln, NE (USA).
- Simeoni, U., & Corbau, C. (2009). A review of the Delta Po evolution (Italy) related to climatic changes and human impacts. *Geomorphology*, *107*, 64–71. <https://doi.org/10.1016/j.geomorph.2008.11.004>
- Smith, L. C., MacDonald, G. M., Velichko, A. A., Beilman, D. W., Borisova, O. K., Frey, K. E., & Kremenetski, K. V. (2004). Siberian peatlands a net carbon sink and global methane source since the early Holocene. *Science*, *303*, 353–356. <https://doi.org/10.1126/science.1090553>
- Stefani, M., & Vincenzi, S. (2005). The interplay of eustasy, climate and human activity in the late Quaternary depositional evolution and sedimentary architecture of the Po Delta system. *Marine Geology*, *222–223*, 19–48. <https://doi.org/10.1016/j.margeo.2005.06.029>
- Terefe, W., Mariscal, S. I., Gomez, M. V., & Espejo, S. R. (2005). Relationship between soil color and temperature in the surface horizon of Mediterranean soils: A laboratory study. *Soil Science*, *170*, 495–503. <https://doi.org/10.1097/01.ss.0000175341.22540.93>
- Terefe, W., Mariscal, S. I., Peregrina, F., & Espejo, S. R. (2008). Influence of heating on various properties of six Mediterranean soils: A laboratory study. *Geoderma*, *143*, 273–280. <https://doi.org/10.1016/j.geoderma.2007.11.018>
- Turner, M. G., Smithwic, E. A. H., Metzger, K. L., Tinker, D. B., & Romme, W. H. (2007). Inorganic nitrogen availability after severe stand-replacing fire in the Greater Yellowstone ecosystem. *Proceedings of the National Academy of Sciences of the United States of America*, *170*, 4782–4789. <https://doi.org/10.1073/pnas.0700180104>
- Uda, S. K., Hein, L., & Atmoko, D. (2019). Assessing the health impacts of peatland fires: A case study for Central Kalimantan, Indonesia. *Environmental Science and Pollution Research*, *26*, 31315–31327. <https://doi.org/10.1007/s11356-019-06264-x>
- Ulery, A. L., Graham, R. C., Chadwick, O. A., & Wood, H. B. (1995). Decade scale changes of soil carbon, nitrogen and exchangeable cations under chaparral and pine. *Geoderma*, *65*, 121–134. [https://doi.org/10.1016/0016-7061\(94\)00034-8](https://doi.org/10.1016/0016-7061(94)00034-8)
- Usup, A., Hashimoto, Y., Takahashi, H., & Hayasaka, H. (2004). Combustion and thermal characteristics of peat fire in tropical peatland in Central Kalimantan, Indonesia. *Tropics*, *14*, 1–19. <https://doi.org/10.3759/tropics.14.1>
- Watts, A. C., & Kobziar, L. N. (2013). Smoldering combustion and ground fires: Ecological effects and multi-scale significance. *Fire Ecology*, *9*, 124–132. <https://doi.org/10.4996/fireecology.0901124>
- Yuan, H., Restuccia, F., & Guillermo, R. (2021). Spontaneous ignition of soils: A multi-step reaction scheme to simulate self-heating ignition of smouldering peat fires. *International Journal of Wildland Fire*, *30*, 440. <https://doi.org/10.1071/WF19128>
- Zethof, J. H. T., Bettermann, A., Vogel, C., Babin, D., Cammeraat, E. L. H., Solé-Benet, A., et al. (2020). Prokaryotic community composition and extracellular polymeric substances affect soil microaggregation in carbonate containing semiarid grasslands. *Frontiers in Environmental Science*, *8*, 51. <https://doi.org/10.3389/fenvs.2020.00051>
- Zethof, J. H. T., Leue, M., Vogel, C., Stoner, S. W., & Kalbitz, K. (2019). Identifying and quantifying geogenic organic carbon in soils – The case of graphite. *Soils*, *5*, 383–398. <https://doi.org/10.5194/soil-5-383-2019>